Physical Modelling of Enclosed Pool Fires—Development of Empirical Correlations

J. P. STENSAAS, P. J. HOVDE, and B. F. MAGNUSSEN[1]
The Norwegian Fire Research Laboratory
SINTEF (Foundation for Scientific and Industrial Research)
The Norwegian Institute of Technology
7034 Trondheim, Norway

ABSTRACT

A series of small-scale enclosed and open pool fire experiments have been carried out in order to study how the fire behavior responds to alterations in the fire conditions in the course of the transient phase of the fire. Empirical correlations have been developed which can serve as a first-hand calculation tool for determining the fire severity of enclosed pool fires (i.e. in terms of the average hot gas layer temperature rise) at any time in the transient phase of the fire when only the parameters of the fire compartment are known.

INTRODUCTION

Fire is a potential risk in offshore installations and onshore process and storage plants. Due to the large amounts of fuel, the rapid development of a fire and the often limited fire fighting resources, such fires represent a special risk to people and property. The fire research activities in Norway have focused attention on hydrocarbon fires during the last ten years. The authorities as well as the Norwegian oil companies Norsk Hydro A/S and Den norske Stats Oljeselskap A/S (Statoil) have sponsored a research programme at SINTEF regarding the modelling of hydrocarbon fires offshore. The project consists of both experimental studies, the development of empirical correlations, and the development of mathematical field models. Experiments have been carried out in a 1:10 scale model of an offshore platform module.

The aim of the project is to develop tools for physical modelling and mathematical calculations in order to characterize important parameters of fire accidents offshore. The tools include experimental facilities, mathematical field and zone models and empirical correlations.

During 1987, a physical model of a platform module in a 1:4 scale will be completed, and this will give the opportunity to establish experimental data both for scaling hydrocarbon fires in enclosures and for the verification of the mathematical models.

---

[1]Division of Thermodynamics, The Norwegian Institute of Technology, The University of Trondheim.

INSTRUMENTATION AND EXPERIMENTAL CONDITIONS[2]

Figure 1 shows the test model compartment with the most important components - frame, fire chamber, and the air distribution system. The dimensions of the model and materials used for the walls, ceiling and floor are noted on the drawing. The pool is comprised of a rectangular pan located in the floor center with the following dimensions (length x width x depth): 500 mm x 50 mm (or 100 mm) x 25 mm. The pan was immersed into the floor and filled with 15 mm of liquid hydrocarbon fuel. The level of hydrocarbon fuel was held approximately constant 10 mm below the floor by supplying fuel from an externally fuel reservoir and an optical regulation system.

The following quantities were measured during the experimental series:

1. Mass evaporation rate of fuel from the pool surface
2. Air supply rate
3. Gas temperatures in the model (51 points)
4. Solid temperatures (31 points)
5. Liquid fuel temperatures (3 points)
6. Exhaust gas concentrations of O_2, CO_2, and CO
7. Thermal heat flux to the floor

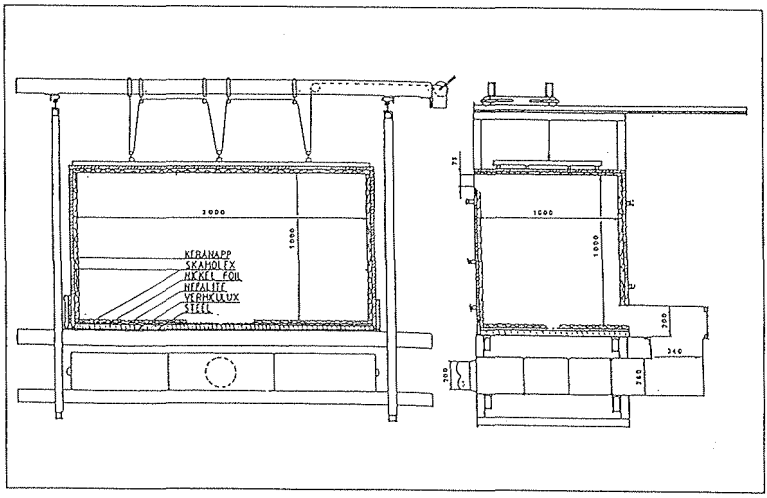

FIGURE 1. The test model (1:10-scale of a platform module). Forced air is introduced along the floor through an air inlet opening of 0.15 m in height and a width extending along the whole length of the model, i.e. approx. 2 m. An air distribution system, which provides an evenly distributed air supply, is connected to this opening. A fan with controllable capacity in front of the air distribution system provides the required air supply. The fire gases exit through the 1 m wide and 75 mm high opening in the middle of the opposite wall by the ceiling.

[2]For a more detailed description of the experimental setup, results and the theory presented in this paper, refer to [1].

The experiments were divided into four experimental series in which only the air supply rate was varied. Table 1 shows that only the size of the pool area or the type of fuel was changed from one experimental series to the next. The only difference between the series termed C and D was that a pipe of 200 mm in diameter and 1 m in length was located 50 mm above the pool surface. From now on each experiment will be symbolized by one of the letters A, B, C, or D in accordance with Table 1, followed by a 2 or 3 digit number representing the air supply rate in g/s.

Experiments with exactly the same pans as used in the model compartment experiments were also carried out in the open with imposed wind toward one long side of the pan in order to simulate the flame configuration of the enclosed pool fire experiments. The pans were immersed into the floor and the liquid level was held constant in the same way as in the enclosed pool fire experiments.

EXPERIMENTAL RESULTS

The Figures 2 and 3 show the mass evaporation rate of fuel per unit pool surface area and the average hot gas layer temperature, respectively. As is evident from these figures the severity of the fire seems to decrease with increasing air supply rates. Evidently due to the cooling effect of the forced air supply. It also appears that the fire developed much more rapidly when the width of the pool was doubled and when the lower boiling point fuel was used.

Evidently the experiment with a steel pipe located close to the pool surface attained the most severe fire condition of all the experiments. It appears also from the Figures 2 and 3 that none of the fire experiments had attained the steady-state phase when they were terminated due to the fact that the internal bounding surfaces (fibre boards) of the fire compartment could not sustain the high fire loads after some time. It must be emphasized that flames were sticking out from the exit opening in all the experiments reported here after a relatively short time, at least when using the largest pan. The external flame plume grew in size

TABLE 1. The experimental conditions.

Experimental series	Pan size (mm)	Fuel depth (mm)	Type of fuel (SBP[3])	Fuel supply temp. (°C)	Boiling point (kJ/kg)	Heat of evaporation (kJ/kg)	Heat of combustion (kJ/kg)	Stoichiometric air to fuel ratio (-)
A	25x50 x500	15±1	140/165	100	144-165	265	43920	15
B	25x100 x500	"	"	"	"	"	"	"
C	"	"	62/82	55	66-74	330	44800	"
D	"	"	"	"	"	"	"	"

[3]Special Boiling Point fuel manufactured by the oil company Shell.

during the experiment. The maximum length of the flame plume was usually in the range 1.5 - 2 m when the experiments were terminated.

Figure 4 shows the heat fluxes to the floor at a point close to the one long side of the pan. It can be seen that the maximum values lie in the range of 25 - 40 kW/m^2. It is reasonable to assume that the heat flux meter receives heat radiation mostly from the hot gas layer due to strong flame distortion away from the flux meter which was a result of the air supply. By calculating the absorbed heat flux to the liquid surface per unit pool surface area to be the sum of the heat required to raise the temperature of the liquid from the supply temperature to boiling point and the heat required to evaporate the fuel, the resultant values will be correspondingly 50 - 80 kW/m^2. The heat of evaporation calculations were based on the mass evaporation rates shown in fig. 2. This should indicate that most of the heat transfer to the fuel bed comes from the flame plume itself.

The mass evaporation rate per unit pool surface area of the experiments in the open is shown in Figure 5. During these pool fire experiments the same two pan sizes and liquid fuels were used as in the enclosed fire experiments. By comparing the maximum values of the enclosed pool fire experiments in Figure 2 with the steady-state values of the experiments in the open air, then it can be seen that the enclosed evaporation rates are roughly twice as large as those in the open. From Figure 2 it appears that practically none of the enclosed pool fire experiments have reached the steady-state value. However, some experiments seem to be approaching the steady state condition at the end of the experiment. Hence, it is not expected that the steady-state values will be significantly larger than the maximum enclosed evaporation rate values of Figure 2. The steady-state evaporation rates of the enclosed pool fire

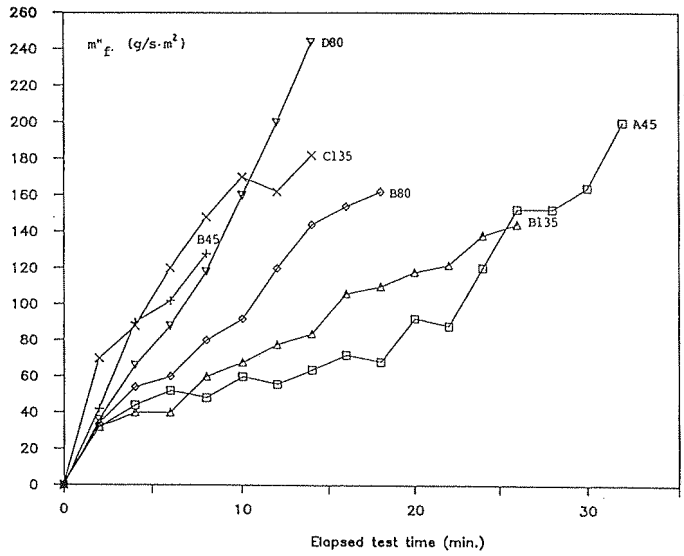

FIGURE 2. The mass evaporation rate of fuel per unit pool surface area, m''_f, under different experimental conditions.

experiments will hardly be more than 2.5 - 3 times the evaporation rates in the open air. This is a considerably lower enhancement of the enclosed evaporation rate compared with the corresponding pool fire experiments of H. Takeda et al. [2] and M.L. Bullen et al. [3], which report a maximum factor of 6 and 7.2, respectively. This must arise from the fact that less sooty fuels must have been used in these experiments leading to a more transparent flame plume and, thus, more radiative heat transfer to the fuel.

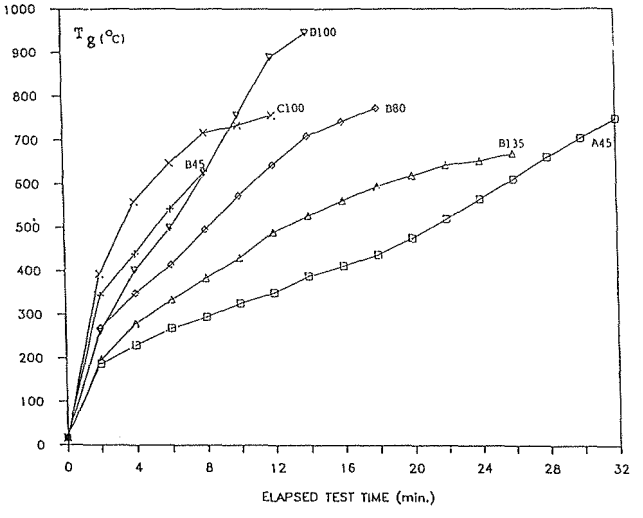

FIGURE 3. The average hot gas layer temperature T_g under different experimental conditions.

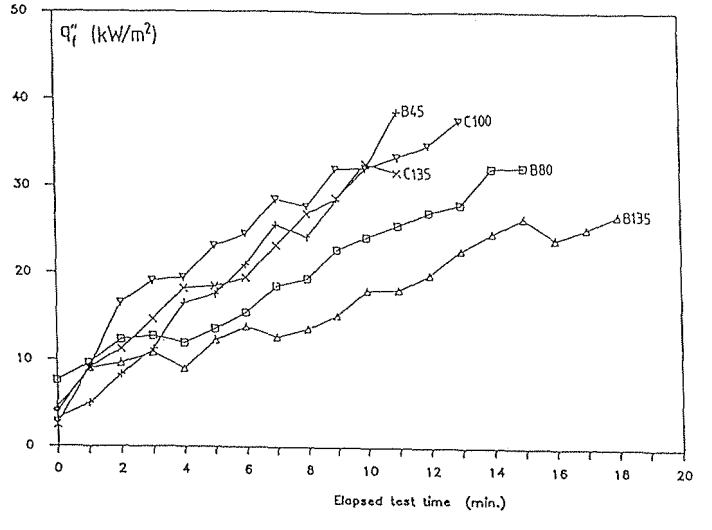

FIGURE 4. The heat flux against the floor, q''_f, at a point 5 cm in front of the middle of the long side of the pan closest to the air inlet.

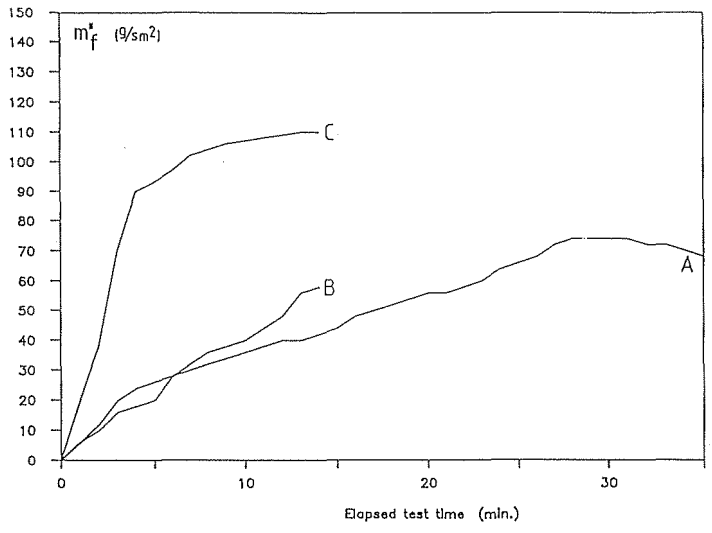

FIGURE 5. The mass evaporation rate of fuel per unit pool surface area in the open air for the same pools as used in the model compartment (The capital letters of the curves refer to the conditions in Table 1.)

In Figure 6 the fuel evaporation rate per unit pool surface area m''_f is plotted as a function of the average hot gas layer temperature increase ΔT_g. The data points of 10 experiments, including one experiment with fire induced air supply, follow the slightly upward convex curve rather well (regression coefficient: 0.94). The mathematical relationship between the parameters mentioned above is also noted in Figure 6. Likewise, in Figure 7, the internal rate of heat release per unit pool surface area q''_{ci} (calculated on the basis of oxygen depletion between the air inlet and the exhaust gas opening) is plotted against the average hot gas layer temperature increase ΔT_g. A regression analysis of the corresponding values of q''_{ci} and ΔT_g yields an exponent equal to 1.4 and a correlation coefficient equal to 0.82. Both the total mass evaporation rate and the internal rate of heat release are proportional to the average hot gas layer temperature increase to the power of 1.4. Hence, this indicates that the ratio of the internal rate of heat release to the total rate of heat release by the fire is roughly constant (equal to approx. 0.6) almost throughout the course of these experiments.

EMPIRICAL CORRELATIONS

The heat balance of the internal volume of the model compartment says that the heat released to the internal volume Q_{ci} is equal to the sum of the ventilation heat loss Q_v, the heat loss to the bounding walls, ceiling, and floor Q_w, the heat radiated through the openings Q_r, and the heat accumulation of the hot upper gas layer Q_a. The two latter terms of the heat balance equation are of minor importance compared to the ventilation heat loss and the wall heat loss. Stensaas [1] has shown that these terms represent more than 95% of the total heat released in the

model compartment regardless of the experimental conditions imposed. Thus, the following approximate expression is then valid:

$$Q_{ci} \approx Q_w + Q_v \qquad (1)$$

The temperature rise, ΔT_g, of the hot gas layer may then be a function of the internal rate of heat release, Q_{ci}, the wall heat loss, Q_w, and the ventilation heat loss, Q_v. On the basis of this approximation above, the following functional relationship can be put forward:

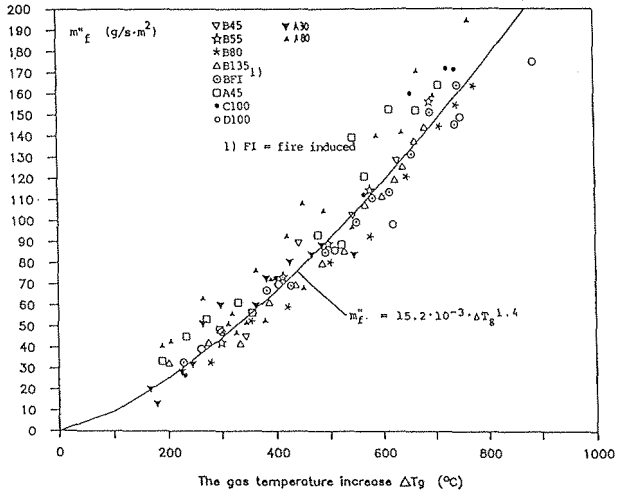

FIGURE 6. The relation between the mass evaporation rate of fuel per unit pool surface area and the temperature rise of the hot gas layer.

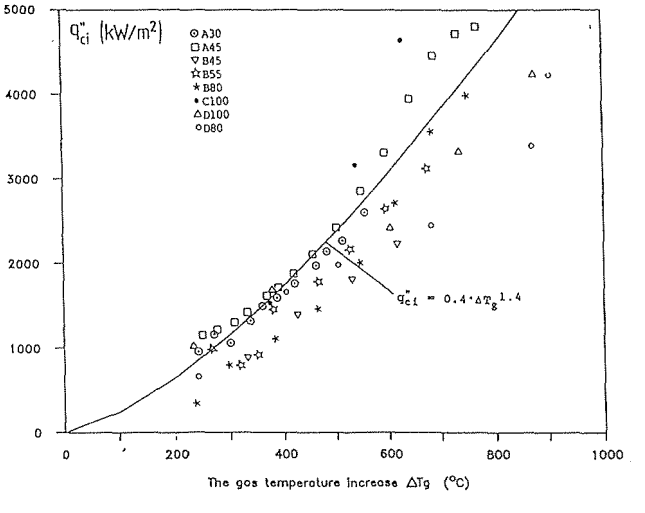

FIGURE 7. The relation between the internal rate of heat release per unit pool surface area, q''_{ci}, and the hot gas temperature rise ΔT_g.

$$\frac{\Delta T_g}{T_o} = c \cdot \left[\frac{Q_{ci}^2}{Q_w \cdot Q_v} \right]^n \qquad (2)$$

where T_o is the initial temperature of the compartment, c is a constant, and n is an exponent greater than zero. The dimensionless function above is reasonable because it implies that the dimensionless temperature rise increases significantly when Q_{ci} increases due to the fact that it is raised to the second power. Further, it appears that the dimensionless temperature rise decreases when both the ventilation heat loss and the heat loss to the enclosing walls increase. The powers of the heat gain and heat loss terms of the dimensionless group are reasonable because, besides forming a dimensionless ratio, it has been shown in [1] that Q_v and Q_w roughly were of the same order of magnitude and that their sum was approximately equal to Q_{ci}. Since it has been shown that the ratio of the internal rate of heat release to the total rate of heat release, Q_{ci}/Q_{ct}, is roughly constant, the internal rate of heat release may be replaced by the total rate of heat release Q_{ct} which is equal to the product of the total mass evaporation rate and the heat of combustion of the fuel. The total mass evaporation rate of fuel, m_f, is an easier parameter to predict rather than the amount of oxygen consumed by the fire. Q_{ct}, Q_v, and Q_w are given by the following relations:

$$Q_{ct} = m_f \cdot \Delta H_c \qquad (3)$$

$$Q_v = m_a c_{pg} \cdot \Delta T_g \qquad (4)$$

$$Q_w = h_w \cdot A_w \cdot \Delta T_w \qquad (5)$$

where m_a is the air supply rate, ΔH_c is the heat of combustion of the fuel, c_{pg} is the specific heat of air, A_w is the wall surface area, and h_w is an effective heat transfer coefficient of the walls, and ΔT_w is the temperature difference of the fluids on each side of the walls. A useful approximation for h_w when assuming a semi-infinite solid with constant surface temperature is, according [4], the expression[4]:

$$h_w = \sqrt{(\rho c_p \lambda)_w / t} \qquad (6)$$

where ρ_w, c_{pw}, and λ_w are the density, specific heat capacity, and thermal conductivity[5], respectively, and t is the actual time of the

---

[4]The procedure for calculating h_w in the case of composite walls, is given in [4].

[5]The following relations between the thermal conductivity, λ, and the average wall temperature, T_{wm}, represent approximate expressions for the thermal conductivity (in kW/mK) of the inner and outer material layers of the walls, respectively:

$$\lambda_i = 4.6 \cdot 10^{-6} (T_{wm} + 273)^{0.54}$$

$$\lambda_o = 1.5 \cdot 10^{-8} (T_{wm} + 273)^{1.32}$$

Likewise, the specific heat (at 1000°C) and density are: 0.84/1.04 kJ/kgK and 350/260 kg/m^3.

transient phase of the fire. Eq. (6) is valid only if the time $t < t_p$, where t_p is the thermal penetration time. It is given by the following approximate expression for a wall with thickness δ (from [4]):

$$t_p = (\rho c_p/k)(\delta/2)^2 \tag{7}$$

By inserting the above expression into the proposed correlation and taking $\Delta T_w \approx \Delta T_g$, we get the following dimensionless correlation after some mathematical manipulations:

$$\frac{\Delta T_g}{T_o} = c' \cdot \left[\frac{m_f^2 \cdot \Delta H_c^2 \cdot \sqrt{t}}{m_a c_{pg} \sqrt{(\rho c_p \lambda)_w} \cdot A_w T_o^2} \right]^{n'} \tag{8}$$

In this group the fuel evaporation rate m_f and the air supply rate m_a are given in kg/s. A regression analysis of the corresponding temperature rise data and the calculated values of the dimensionless group yields the correlation shown in Figure 8 (the dimensionless group within the parenthesis of Eq. (8) is here termed Y). The regression analysis yields a correlation coefficient slightly above 0.96.

An objection to this empirical correlation is that it includes a dependent variable, namely the total mass burning rate of fuel, m_f. By inserting the functional relationship between the total mass evaporation rate of fuel and the temperature rise given in Figure 6 into the correlations in Figure 8, this dependent variable will be eliminated. After some mathematical manipulations the result will be the following dimensionless correlation for the temperature rise of the hot gas layer:

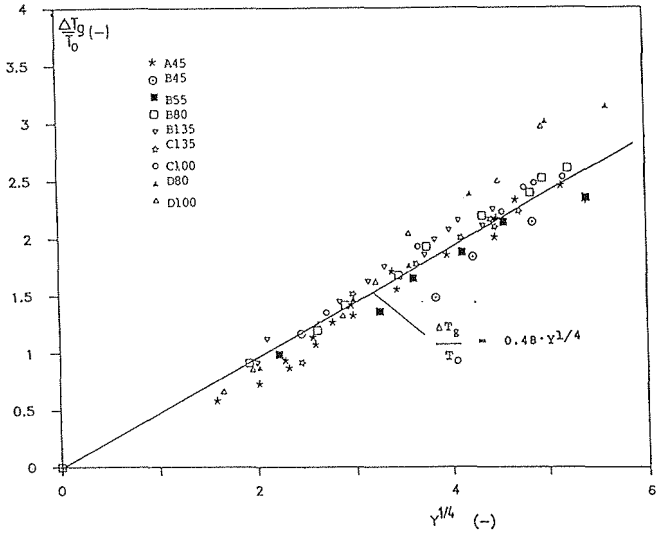

FIGURE 8: The hot gas layer temperature rise as a function of the dimensionless group Y raised to the 1/4-power.

$$\frac{\Delta T_g}{T_o} = 8.1 \cdot 10^{-10} \cdot \left[\frac{A_p^2 \Delta H_c^2 \sqrt{t}}{m_a c_{pg} \sqrt{(\rho c_p \lambda)_w} A_w T_o^{4/5}} \right]^{5/6} \quad (9)$$

CONCLUSIONS

Highly transient burning behavior was observed in all the fire experiments and there was a considerable amount of combustion taking place outside the exit opening during the last part of the experiments. Generally, the fire developed far more rapidly by doubling the pool area, by using the lower boiling point fuel, or by decreasing the air supply rate. The fire severity was obviously at its greatest when a large steel pipe was placed in the proximity of the pool surface. The fuel evaporation rates of the pool fire experiments in the open air with the same pan sizes and types of liquid fuels were approximately half the enclosed evaporation rates.

It has been shown that both the total mass evaporation rate of fuel per unit pool surface area and the internal rate of heat release are proportional to the temperature increase of the hot gas layer to the power of 1.4. Hence, it was concluded that the ratio of the internal rate of heat release to the total rate of heat release was fairly constant almost throughout the course of these fire experiments.

An empirical correlation for the average temperature rise of the hot gas layer has been developed on the basis of this experimental series. The dimensionless temperature rise seems to correlate well with a power law function of the dimensionless ratio of the total rate of heat release to the second power to the product of the ventilation heat loss and the wall heat loss. By inserting the predicted functional relationship between the mass evaporation rate of fuel per unit pool surface area and the average temperature increase of the hot gas layer into this correlation, the resultant expression only contains the given parameters of the model compartment. Hence, the temperature rise of any ventilated compartment pool fire can be predicted at any time of the transient phase of the fire directly from the physical dimensions, material properties of the compartment and the rate of ventilation.

ACKNOWLEDGEMENTS

The authors wish to gratefully acknowledge the help by research engineers Øivin Brandt, who has been responsible for the construction of the model compartment and the instrumentation, and Kristen Opstad who has been responsible for the data acquisition and data reduction. This project was financially supported by the Norwegian oil companies Den norske Stats Oljeselskap A/S (Statoil) and Norsk Hydro A/S as well as The Royal Norwegian Council of Scientific and Industrial Research.

NOMENCLATURE

A	area (m^2)
c, c'	constants (-)
c_p	specific heat (kJ/kg·K)

ΔH_c heat of combustion of the fuel (kJ/kg)
h_w effective heat loss coefficient of the walls (kW/m^2K)
m_f fuel mass flow rate (g/s) (given kg/s in the dimensionless group of Eq. (4), (8) - (10)).
m_a air supply rate (g/s) (")
m_f'' mass evaporation rate of fuel per unit pool surface area ($g/s \cdot m^2$)
n, n' exponents (-)
Q heat flow rate (kW)
q" heat flow rate per unit area (kW/m^2)
T temperature (K)
ΔT temperature increase or difference (K)
t time (s)
Y the ratio of the total heat produced by the fire to the second power and the product of the wall heat loss and the ventilation heat loss (-)

Greek letters:

λ thermal conductivity (kW/mK)
ρ density (kg/m^3)

Subscripts:

a air
c combustion, convective
f fuel, floor
g gas
i internal
o initial
p pool
s stored
t total
v ventilation
w walls, ceiling, floor

REFERENCES

1. Stensaas, J.P.: Physical Modelling of Enclosed Pool Fires - Thesis for the Degree Doctor of Engineering, Division of Thermodynamics, The Norwegian Institute of Technology, The University of Trondheim, The Norwegian Fire Research Laboratory - SINTEF, 1987.

2. Takeda, H and Akita, K.: Critical Phenomenon in Compartment Fires with Liquid Fuels, 18th Symposium (Int.) on Combustion, The Combustion Institute, Pittsburgh, 1981.

3. Bullen, M.L. and Thomas P.H.: Compartment Fires with Non-Cellulosic fuels, 17th Symposium (Int.) on Combustion, The Combustion Institute, Pittsburgh, 1979.

4. McCaffrey, B.J., Quintiere, J.G., Harkleroad, M.F.: Estimating Room Temperatures and the Likelihood of Flashover Using Fire Test Data Correlations, Fire Technology, Vol. 17, No. 2, p. 98, May 1981.